

# Conductivity, Dielectric Relaxation And Structural Studies Of PEO Complexed With Lithium Acetate And Lithium Triflate Salts

Leeana Ismail, L.P. Teo and A.K. Arof

Center for Ionics University of Malaya, Department of Physics, Faculty of Science, University of Malaya, 50603 Kuala Lumpur, Malaysia

Corresponding author: [akarof@um.edu.my](mailto:akarof@um.edu.my)

## Abstract

Polyethylene oxide (PEO) films doped with lithium acetate (LiOAc) and lithium triflate (LiOTf) were prepared by the solution cast technique. Lithium acetate was added to PEO at different weight ratios ranging from 0 wt. % to 30 wt. % whereas lithium triflate concentration was varied from 0 wt. % to 14 wt. %. The polymer-salt solutions were cast in different glass containers and left to dry until the films have formed. The samples were then characterized by electrical impedance spectroscopy (EIS) to obtain the electrical conductivity and to determine the dielectric properties of both systems. The highest room temperature electrical conductivity obtained for PEO-LiOAc system is  $2.18 \times 10^{-6} \text{ S cm}^{-1}$  for the sample containing 30 wt. % lithium acetate and  $8.22 \times 10^{-6} \text{ S cm}^{-1}$  for PEO-LiOTf system at 12 wt. % concentration of lithium triflate. From the Argand plots, it was found that the relaxation process in PEO-LiOAc system is attributed to the viscoelastic relaxation and for PEO-LiOTf system, it is due to conductivity relaxation.

**Keywords:** polyethylene oxide, ionic conductivity, lithium salts, dielectric relaxation, conductivity relaxation

## 1. INTRODUCTION

The study of solid polymer electrolytes has become very popular among researchers because of its potential applications in electrochemical devices such as rechargeable lithium batteries, supercapacitors, electrochromic windows and sensors [1-4]. These polymeric electrolytes are easy to prepare in thin film form and are able to form effective electrode-electrolyte contacts [5]. Most of the studies in polymer electrolyte are devoted to polyethylene oxide (PEO) and polypropylene oxide (PPO) using alkali metal salts such as  $\text{LiBF}_4$ ,  $\text{LiPF}_6$  [6],  $\text{LiCF}_3\text{SO}_3$ ,  $\text{LiClO}_4$  [7],  $\text{NaSCN}$  and etc [8]. The interest in these polymer electrolytes has been widely studied since Wright and co-workers [9] and Armand and co-workers [10] discovered that polyethylene oxide (PEO)-salt

complexes [11-12] can support ionic conductivity. Since then, many other polymeric materials have been tested and found to exhibit ionic conductivity. PEO is used in this work as the polymer host for ionic conduction as it can solvate many types of salt [13]. In PEO polymer electrolyte, cations of ionic salts are coordinated with the ether oxygen of PEO. Changing the chemical composition can vary the physical properties. The polymer chain motion plays a significant role in ionic conduction [13].

In this work, lithium acetate (LiOAc) and lithium triflate (LiOTf) were used as salts to give  $\text{Li}^+$  transporting ions in the electrolytes. The complexation between PEO-LiX (X is the anion of the salt after dissociation) has been reported to increase the amorphous phase of the electrolyte.

increase in amorphous domain of polymer has been reported to result in conductivity enhancement [14]. According to Kumar and Sekhon [14], the addition of salt causes a decrease in the degree of crystallinity of the polymer. In other words, the addition of salt has increased the amorphousness of the polymer and thereby helps to increase the conductivity. The diffraction peaks observed at  $2\theta$  angles are tending to be less intense in complexed polymer-salt films compared to the pure polymer films. In general, solid polymer electrolytes have amorphous and crystalline phases which are contributed from polymer-salt complex domain and the uncomplexed crystalline polymer domain [15]. The surface of PEO-salt complexes have spherulite structures. Pereira et al. [16] reported that the surface morphology in polymer blends based on PEO and starch exhibit spherulite structures.

From impedance data, dielectric data can be calculated. From such data, the relaxation process viz., viscoelastic relaxation and conductivity relaxation [17-20] can be determined. Viscoelastic relaxation is the relaxation of permanent dipoles present on the side chains of the polymer backbone. Conductivity relaxation is due to translational diffusion of ions which results in charge transportation.

## 2. EXPERIMENTAL

### 2.1 Sample Preparation

Polyethylene oxide (PEO) with molecular weight  $3 \times 10^5 \text{ g mol}^{-1}$  was used as the polymer host. 1 g of PEO and different concentrations (wt. %) of LiOAc were mixed in 50 ml 1% acetic acid solution. For the PEO-LiOTf system, the solvent used was acetonitrile. The mixtures were continuously stirred with a magnetic stirrer for several hours at room temperature.

When complete dissolution is achieved, the solutions were cast into different glass containers and left to dry at room temperature until the films have formed. The amounts of lithium acetate and lithium

triflate added were varied from 0 to 30 wt. % and 0 to 14 wt. %, respectively. Above 30 wt. % and 14 wt. %, the PEO-LiOAc and PEO-LiOTf films cannot be peeled easily.

### 2.2 Impedance Spectroscopy

The impedance of the samples was measured for both systems, with a HIOKI 3531-01 LCR Hi-tester. This bridge has been set to measure the impedance and phase angle from 50 Hz to 1 MHz. The impedance measurements were performed from room temperature (25 °C) until 100 °C at 10 °C regular intervals. The software controlling the measurements also calculates the real and imaginary impedance.

The imaginary impedance is usually negative indicating the sample to be capacitive. From the complex impedance plot, the bulk resistance ( $R_b$ ) can be obtained and the electrical conductivity calculated following the method shown in the literature [21-23].

### 2.3 Dielectric Relaxation Studies

The dielectric properties at every frequency were calculated using impedance data. The value of real modulus ( $M'$ ), imaginary modulus ( $M''$ ), dielectric constant ( $\epsilon'$ ) and dielectric loss ( $\epsilon''$ ) were calculated from the imaginary and real impedance data according to

$$\epsilon' = \frac{-\omega C_c Z''}{(\omega C_c)^2 \left[ (Z')^2 + (Z'')^2 \right]} \quad (1)$$

$$\epsilon'' = \frac{j\omega C_c Z_r}{(\omega C_c)^2 \left[ (Z')^2 + (Z'')^2 \right]} \quad (2)$$

$$M' = -\omega C_c Z'' \quad (3)$$

$$M'' = j\omega C_c Z' \quad (4)$$

From the values calculated, Argand plots were constructed for both systems and the relaxation process were then determined from the shape of the  $M_r$ -frequency plots.

2.4 Scanning Electron Micrographs (SEM)

SEM studies were carried out to determine the surface morphology of the samples in both systems.

3. RESULTS AND DISCUSSION

From the impedance measurements taken at various temperatures, the conductivity for all samples from 25 °C until 100 °C was obtained. Fig. 1 and Fig. 2 show the plots of conductivity versus reciprocal temperature for both systems.

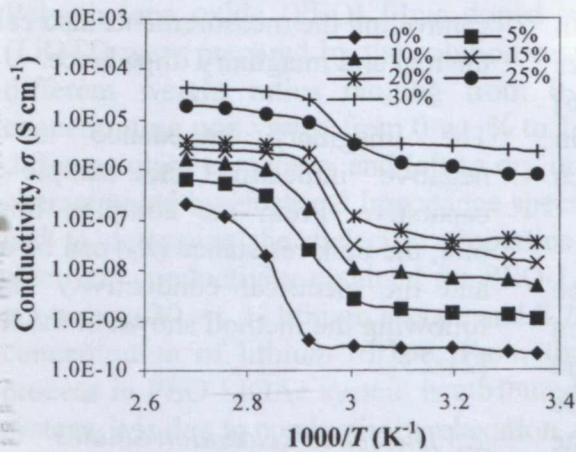


Fig. 1 Plot of conductivity ( $S\text{ cm}^{-1}$ ) versus  $1000/T\text{ (K}^{-1}\text{)}$  for PEO-LiOAc system

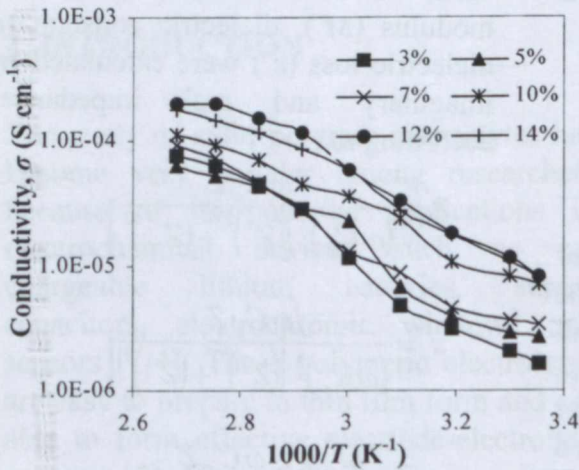


Fig. 2 Plot of conductivity ( $S\text{ cm}^{-1}$ ) versus  $1000/T\text{ (K}^{-1}\text{)}$  for PEO-LiOTf system

It can be observed that the shape of the conductivity-temperature plot for the PEO-LiOAc system is different from that of the PEO-LiOTf system. Fig. 1 shows that the conductivity,  $\sigma$  undergoes an abrupt increase between 333 and 353 K. This is attributed to the phase transition of PEO which melts at

$\sim 340\text{ K}$  for the PEO-LiOAc system. The results are similar to that observed Mohan et al. [5] for the PEO-NaBiF<sub>4</sub> system. The same pattern conductivity-temperature variation are also observed by Sreekanth et al. [24] and Kurian et al. [13] in which the melting temperature  $T_m$  is within the same region. The increase in conductivity with temperature for the PEO-LiOTf system does not show such abrupt change.

On the microscopic scale, at melting temperature/process, there is an increase in the amorphous phase. Due to this increase the conductivity increased at  $T_m$ . The highest electrical conductivity at room temperature for PEO-LiOAc and PEO-LiOTf systems is  $2.18 \times 10^{-6}\text{ S cm}^{-1}$  and  $8.22 \times 10^{-6}\text{ S cm}^{-1}$ , respectively.

Dielectric analysis was carried out to determine whether relaxation process is due to viscoelastic relaxation or due to conductivity relaxation. Fig. 3 and Fig. 4 show the Argand plots for the high conducting sample for both systems at room temperature.

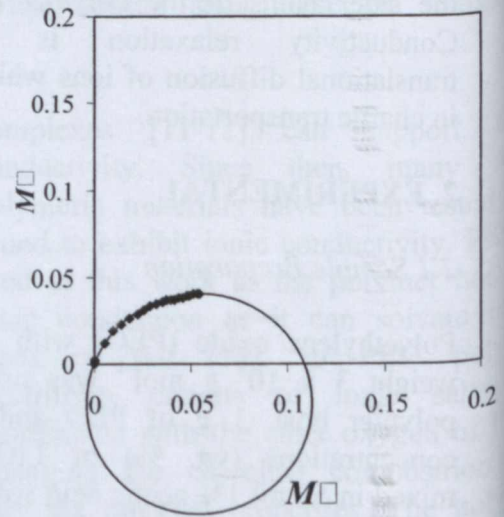


Fig. 3 Argand plot for PEO-LiOAc system

The Argand plots illustrate the shape of a semicircle for each system. For the PEO-LiOAc system the semicircle is tilted with its centre at the bottom of the horizontal axis, indicating that the relaxation process is due to viscoelastic relaxation process. For the PEO-LiOTf system, the relaxation process is due to conductivity relaxation process [17].

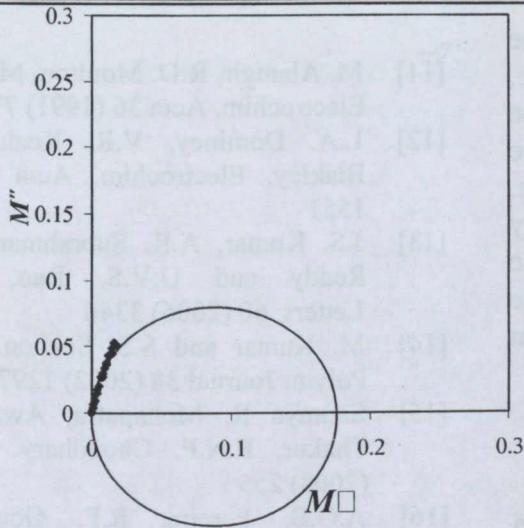


Fig. 4 Argand plot for PEO-LiOTf system

According to Mohamed et al. [17], the real and imaginary electrical modulus are related to the relaxed modulus,  $M_R$  and unrelaxed modulus,  $M_u$  via the equation

$$\left\{ M' - \frac{M_u + M_R}{2} \right\}^2 + (M'')^2 = \left( \frac{M_u - M_R}{2} \right)^2 \quad (5)$$

If  $M_u = 0$ , then

$$M_R = \frac{(M')^2 + (M'')^2}{M'} \quad (6)$$

Substituting the values of  $M'$  and  $M''$  obtained for every frequency into Equation (5), then the ratio of the right hand side (RHS) value to the left hand side (LHS) value should be equal to one if the plot is a perfect semicircle. Fig. 5 shows the LHS to RHS ratio,  $X$  versus frequency.

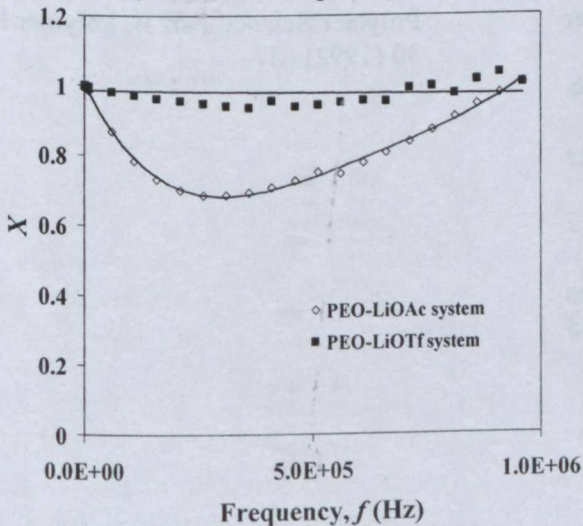
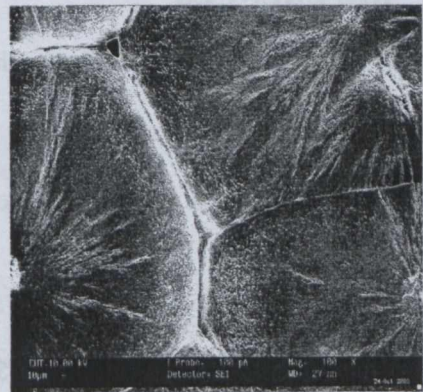


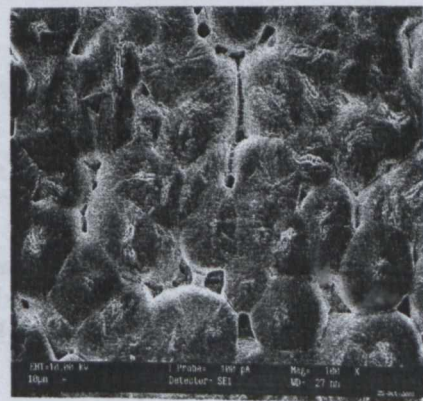
Fig. 5 Plot of  $X$  versus frequency,  $f$  (Hz)

It can be seen that the plot for the first system, PEO-LiOAc does not show any semicircular shape because the LHS to the RHS ratio varies with frequency. Hence, the dielectric relaxation is viscoelastic relaxation. Viscoelastic relaxation in such ionic conductors, exhibit multiple relaxation times [25]. For the second system, PEO-LiOTf,  $X$  versus frequency is almost constant and the values fluctuate about one. This is indicative that the plot exhibits a semicircular shape.

Fig. 6 (a) and (b) show the surface morphology for the PEO film formed by dissolving PEO powder in 1% acetic acid solution and that of a PEO film formed by dissolving PEO powder in acetonitrile, respectively.



(a)



(b)

Fig. 6 SEM micrographs of PEO formed by dissolving PEO in (a) 1% acetic acid and (b) acetonitrile

It can be observed that the shapes of the spherulites are different. In the PEO-LiOAc, system the spherulites have a polygon shape and in the PEO-LiOTf system, the spherulites have a cell type microstructure. This is attributed to the different solubility rate of PEO in the two solvents and also the evaporation rate of the solvents. Existence of pores is due to uncontrolled evaporation of the solvents.

#### 4. CONCLUSIONS

The polymer electrolyte PEO-LiOAc system exhibit a distribution of relaxation times. This is characterized by their Cole-Cole plot ( $M''$  versus  $M'$ ). For the PEO-LiOTf system, the relaxation process is conductivity relaxation. The type of solvent affects the surface morphology of the systems.

#### REFERENCES

- [1] P.V. Wright. *Electrochim. Acta* 43 (1998) 1137
- [2] G. Casalbore-Miceli, N. Camaioni, M.J. Yang, M. Zhen, X.W. Zhan and A. D'Aprano. *Solid State Ionics* 10 (1997) 217
- [3] M.Z.A. Yahya and A.K. Arof. *European Polym. Journal* 38 (2002) 1191
- [4] M.Z.A. Yahya and A.K. Arof. *Carbohydrate Polymers* 55 (2004) 95
- [5] V. Madhu Mohan, V. Raja, A.K. Sharma and V.V.R. Narasimha Rao. *Materials Chemistry & Physics* 94 (2005) 77
- [6] H. Devendrappa, U.V. Subba Rao, and M.V.N. Ambika Prasad. *J. Power Sources* 155 (2006) 368
- [7] D. Fautex and C. Robitaille. *Electrochem. Soc.* 133 (1986) 307
- [8] H. Zhang and J. Wang. *Spectrochimica Acta Part A*, 71 (2009) 1927
- [9] P.V Wright. *British Polymer Journal* 7 (1975) 319
- [10] M.B. Armand, In *Polymer Electrolytes Review I*, (Eds.) MacCallum, J.R. and Vincent, C.A., Elsevier, U.K. (1987) 1
- [11] M. Alamgir, R.D. Moulton, M. Abramo. *Electrochim. Acta* 36 (1991) 773
- [12] L.A. Dominey, V.R. Kosh and Blakley. *Electrochim. Acta* 37 (1992) 1551
- [13] J.S. Kumar, A.R. Subrahmanyam, Reddy and U.V.S. Rao. *Materials Letters* 60 (2006) 3346
- [14] M. Kumar and S.S. Sekhon. *European Polym. Journal* 38 (2002) 1297
- [15] Saumya R. Mohapatra, Awalendra Thakur, R.N.P. Choudhary. *Ionics* (2008) 255
- [16] A.G.B. Pereira, R.F. Gouveia, C. Carvalho, A.F. Rubira, E.C. Muniz. *Materials Science and Engineering C* (2009) 499
- [17] K. Mohamed., T.G. Gerasimov, Moussy, and J.P. Harmon. *Polymer* (2005) 3847
- [18] M.M. El-Nahass, A.M. Farid, K.F. Al-El-Rahman and H.A.M. Ali. *Physica B* 403 (2008) 2331
- [19] B.K. Choi, Y.W. Kim. *Electrochim. Acta* 49 (2004) 2307
- [20] A.S. Ayesh. *J. Thermoplastic Composite Materials* 21(2008) 309
- [21] M.J. Reddy, J.S. Kumar, U.V. Rao, and Peter P. Chu, *Solid State Ionics* 177 (2006) 253
- [22] F. Croce, S. Sacchetti and B. Scrosati. *Power Sources* 161 (2006) 560
- [23] C.W. Lin, C.L. Hung, M. Venkateswari and B.J. Hwang. *J. Power Sources* (2005) 397
- [24] T. Sreekanth, M.J. Reddy, Subramanyam and U.V.S. Rao, *Materials Science and Engineering B* 64 (1999) 105
- [25] H.W. Starkweather Jr and P. Avakian. *Polymer Science Part B, Polymer Physics* 30 (1992) 637